

Self-sustained activity, bursts, and variability in recurrent networks

Marc-Oliver Gewaltig^{1,2}

1) Blue Brain Project, École Polytechnique Fédérale de Lausanne, QIJ, CH-1015 Lausanne, Switzerland

2) Honda Research Institute Europe GmbH, D-63073 Offenbach, Germany

E-mail: marc-oliver.gewaltig@epfl.ch

Abstract

There is consensus in the current literature that stable states of asynchronous irregular spiking activity require (i) large networks of 10 000 or more neurons and (ii) external background activity or pacemaker neurons. Yet already in 1963, Griffith showed that networks of simple threshold elements can be persistently active at intermediate rates. Here, we extend Griffith's work and demonstrate that sparse networks of integrate-and-fire neurons assume stable states of self-sustained asynchronous and irregular firing without external input or pacemaker neurons. These states can be robustly induced by a brief pulse to a small fraction of the neurons, or by short a period of irregular input, and last for several minutes. Self-sustained activity states emerge when a small fraction of the synapses is strong enough to significantly influence the firing probability of a neuron, consistent with the recently proposed long-tailed distribution of synaptic weights. During self-sustained activity, each neuron exhibits highly irregular firing patterns, similar to experimentally observed activity. Moreover, the interspike interval distribution reveals that neurons switch between discrete states of high and low firing rates. We find that self-sustained activity states can exist even in small networks of only a thousand neurons. We investigated networks up to 100 000 neurons. Finally, we discuss the implications of self-sustained activity for learning, memory and signal propagation.

Author Summary

Neurons in many brain areas are active even in the absence of a sensory stimulus. Many models have tried to explain this *spontaneous activity* by spiking activity, reverberating in recurrent networks of excitatory and inhibitory neurons. But so far the conclusions have been that such networks can only sustain spontaneous activity under certain conditions: The networks must be large and there must be either endogenously firing neurons (so called *pacemaker neurons*) or diffuse external input which keeps the network active. Here we show that recurrent networks of excitatory and inhibitory neurons can sustain spontaneous activity for periods of many minutes, provided that a small percentage of the connections are sufficiently strong. Thus, contrary to previous findings, self-sustained (spontaneous) activity does neither require large networks nor external input or pacemaker neurons. The spike patterns observed during self-sustained activity are chaotic and highly irregular. The interspike interval distribution during self-sustained activity reveals that the network switches between different discrete states, each characterized by their own time scale. Our results provide a possible explanation of self-sustained cortical activity and the role of the recently observed long-tailed weight distributions in the mammalian cortex.

Introduction

Spontaneous activity, that is, activity in the absence of a sensory stimulus, is a ubiquitous phenomenon in the brain that has puzzled generations of researchers. Spontaneous activity is highly irregular and has a strong effect on evoked neuronal responses [1, 2]. In fact many researchers argue that this *ongoing activity* represents information rather than noise [3, 4]. Moreover, spontaneous activity in the cortex is

stable and robust and can be observed in awake as well as in anesthetized animals throughout their entire life.

It is commonly assumed that spontaneous activity is created by reverberating activity within recurrent neuronal circuits, but the exact mechanisms by which neurons maintain their low rate firing are still not well understood.

Already in 1956 Beurle showed that networks of excitatory neurons (“a mass of units capable of emitting regenerative pulses”) generally have an inherently unstable activity in which all or none of the units are excited [5].

In 1962 Ashby and co-workers [6] reproduced Beurle’s findings under more simplified assumptions and delivered a mathematical proof for the instability of recurrently connected excitatory threshold units. They derived an expression for the probability of an output pulse as function of the probability for an input pulse and showed that this function takes the form of the now well known sigmoid. They concluded that “the more richly organized regions of the brain offer us something of a paradox. They use threshold intensively, but usually transmit impulses at some moderate frequency, seldom passing in physiological conditions into total inactivity or maximal excitation. Evidently there must exist factors or mechanisms for stability which do not rely on fixed threshold alone” [6].

In 1963 Griffith extended the models of Beurle [5] and Ashby [6] in two ways. First, he remarked that networks with dedicated connectivity can support stable states of low or intermediate firing rates. For example the *complete transmission line* consists of consecutive groups of neurons that are connected by diverging/converging connections. In such a network, activity will travel unperturbed from one group to the next, without exciting the entire network. This network architecture became later known as the *synfire chain* [7].

The second addition of Griffith were inhibitory neurons which Ashby had neglected. Griffith also found that networks of excitatory and inhibitory neurons don’t support stable states at low or intermediate levels of activity if the neurons have many excitatory and inhibitory inputs with correspondingly small synaptic weights.

He then went on to show that for the special case of a few synaptic inputs per neuron, such stable activity states should indeed exist. Since computational power in 1963 was more limited than it is today, he restricted his analysis to the case of few excitatory inputs with global inhibition, i.e. and one inhibitory input, strong enough to suppress the combined input of all excitatory neurons. In this case, activity is stable at an intermediate rate. This suggests that stable, low or intermediate firing rates should exist for more realistic network configurations.

Thirty years later, van Vreeswijk and Sompolinski revived interest in self-sustaining activity in recurrent networks with two seminal papers [8,9] in which the authors introduced the concept of *balanced excitation and inhibition* as a criterion for the emergence of stable activity states. But in their model, external input is needed to obtain stable activity at low or intermediate rates.

Since then several studies have shown that self-sustained activity is possible under some conditions. In recurrent networks of *conductance based* neurons, self-sustained activity can survive for a limited time [10,11]. Otherwise additional activating mechanisms, like external input or [12,13], endogeneously firing neurons [14,15], or cells which respond to an *inhibitory* stimulus [16], are needed to sustain activity.

Moreover, self-sustained activity in recurrent network models is still too regular compared to experimental data [17,18] and additional *de-correlating* mechanisms are needed [19].

In this paper we show that highly irregular self-sustained activity is an inherent property of recurrent neural networks with excitation and inhibition. These states occur in relatively small networks (one thousand neurons and more) if the connectivity is sparse and the connection strengths is large.

Self-sustained activity can be robustly induced by a brief pulse to a small fraction of the neurons. We will show that these self-sustained states differ in their survival time statistics and their interspike interval distributions from previously reported self-sustained states.

In the following section, we will briefly revisit the results of Ashby [6] and Griffith [20] to show

under which conditions recurrent networks of excitatory and inhibitory neurons can sustain states of low rate almost indefinitely. We will then investigate the nature and properties of these states in computer simulations. We demonstrate that self-sustained activity, even in small networks is stable and long-lived, provided the connectivity is sparse and synapses are strong. We compare self-sustained activity with the asynchronous irregular state (AI state), characterized by Brunel [13]. We find that the firing patterns of neurons in the self-sustained states are highly irregular. This irregularity can be seen in the wide range of firing rates and large coefficients of variation (CV) of the interspike intervals. While self-sustained activity states require sparse and strong connections, the required post-synaptic potential (PSP) amplitudes are still in the physiological range. Moreover, self-sustained activity states emerge in weakly coupled networks with a few strong connections, corresponding to the recently proposed idea that cortical connectivity is best described as a few strong synapses in a sea of weak ones [21] or a long-tailed distribution of synaptic weights.

Results

Stability in networks of simple threshold elements

Following Ashby [6], we describe the activity of a neuron by a single number p which satisfies $0 \leq p \leq 1$ and which is the probability of observing a spike in a sufficiently small interval Δt :

$$p = \lim_{t \rightarrow \infty} \left(\frac{n}{C} \cdot \frac{\Delta t}{t} \right) \quad (1)$$

where n is the number of spikes arriving at the inputs C at time t . The probability of observing exactly n spikes on the C inputs follows a binomial distribution:

$$p_n = \binom{C}{n} p^n (1-p)^{C-n} \quad (2)$$

Now assume that a neuron fires, if there are $n \geq \theta$ input spikes. Then the probability for producing an output spike is given by the cumulative binomial probability function:

$$P(p) = \sum_{n=\theta}^C \binom{C}{n} p^n (1-p)^{C-n} \quad (3)$$

We can estimate the long-term behavior of the network activity by considering equation (3) as an iterative map. Starting from an initial activity p_0 , we repeatedly apply (3). Ashby found, that the only stable fixed points in this iteration are $p = 0$ and $p = 1$, that is, either all the neurons are silent or all neurons are active. Griffith [20] noted that this situation changes if the network also contains inhibitory neurons. In the case of C_E excitatory and C_I inhibitory inputs, the new threshold condition becomes:

$$n_E - g \cdot n_I \geq \theta \quad (4)$$

where n_E is the number of spikes at the C_E excitatory inputs and n_I the number of spikes at the C_I inhibitory inputs, and g a factor that captures the difference in synaptic efficacies. To reflect the cortical ratio of 80% excitatory neurons to 20% inhibitory neurons, we choose:

$$C_I = \gamma \cdot C_E$$

with $\gamma = 0.25$.

To obtain the probability for passing the threshold, we must now consider the joint probabilities for observing n_E excitatory and n_I inhibitory spikes. The respective cumulative probability function given by:

$$P(p) = \sum_{n_E - g \cdot n_E \geq \theta} \binom{C_E}{n_E} \binom{C_I}{n_I} p^{n_E + n_I} q^{C_E + C_I - n_E - n_I} \quad (5)$$

where $q = 1 - p$ and the sum is over all combinations of n_E and n_I that satisfy the threshold condition (4). Again, we can use this expression as an iterative map to determine whether a given probability p is stable under repeated application of equation (5), that is:

$$p^* = p = P(p) \quad (6)$$

with the condition that

$$\left| \left(\frac{\partial P(p)}{\partial p} \right)_{p^*} \right| < 1 \quad (7)$$

Griffith showed that no stable activity exists, if C_E and C_I become large. But, if the number of inputs is small and the inhibitory efficacy is very strong, then there is a stable solution at $p = 1/2$. Griffith solved equation (5) for the case of global inhibition which is strong enough to suppress an output spike, even if all excitatory inputs are active.

Unfortunately, it is not easy to determine whether other stable solutions to equation (5) exist, because the equation is discrete and involves the binomial coefficients of all possible input combinations that reach or exceed threshold. Typical approximations use the assumptions that the number of inputs is large and the individual probabilities are low. Then, the law of large numbers allows us to replace the binomial distribution with a normal distribution. Unfortunately, these are the conditions for which we already know that all solutions are unstable [20] and that external input is needed to obtain self-reproducing activities [9, 12, 13].

In this paper we won't attempt to simplify equation (5) further, but rather we will investigate it numerically. We will demonstrate that for sparse networks with large synaptic efficacies, there indeed exist stable self-sustaining activity states. We will then investigate these states in large-scale network simulations of current based integrate-and-fire neurons. In a companion paper by Enger et al. (2013) we derive a theory which explains self-sustained activity states as well as their survival times.

Many inputs and high-threshold

Neurons in cortex have a large number of synapses [22, 23] and it is often assumed that this also implies that the individual synapses must be small [23], that is, the threshold is large. Unfortunately, it is difficult to reach threshold under these conditions, because a large number of neurons must be simultaneously active. This is reflected in the very low output probability for this situation. Figure 1A shows the numerical solution of equation (5) for a network with $C_E = 1000$, $C_I = 250$, $\theta = 100$. The probability stays orders of magnitudes below the diagonal and the only stable fixed-point is $P(0.0) = 0.0$.

Incidentally, these parameters are used by Brunel [13] for the asynchronous irregular activity state. Since the output probability is low, the asynchronous irregular state requires an external input that lifts the output probability above the diagonal.

The only way to increase the firing probability without adding external input is to lower the firing threshold. In figure 1B, the threshold is only half as high at $\theta = 50$ and as a result the peak probability has increased by a factor of almost 1000, but the curve is still far below the diagonal.

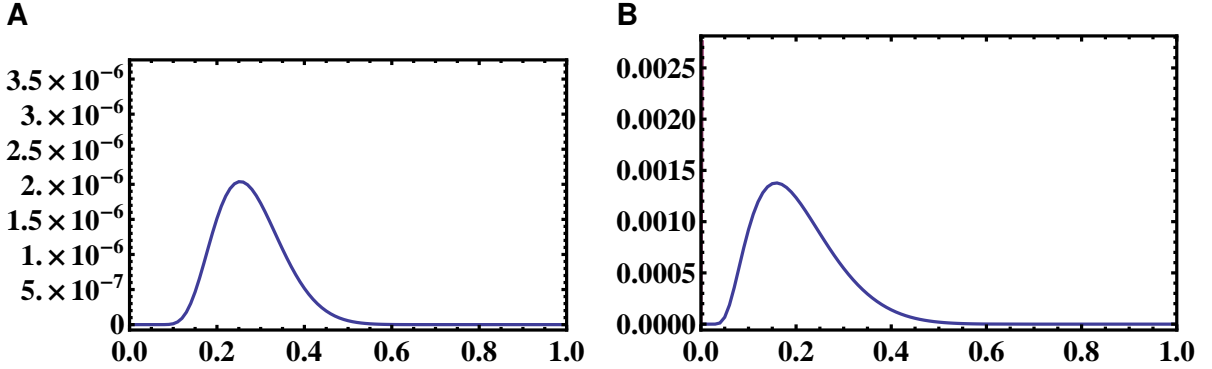


Figure 1. Effect of the firing threshold on the firing probability transfer function (numerical solution of equation (5)) **(A)** Many synapses, high threshold; $\theta = 100, C_E = 1000, C_I = 250$. The probability stays orders of magnitudes below the diagonal and the only stable fixed-point is $P(0.0) = 0.0$. **(B)** Many synapses, lower threshold; $\theta = 50, C_E = 1000, C_I = 250$. The peak probability is increased by almost three orders of magnitude.

Stability with low threshold

The threshold has a strong non-linear influence on the firing probability, because the odds of finding sufficiently many coincident (or near coincident) spikes decrease at least exponentially with increasing threshold. We can use this lever to our advantage and lift the firing probability above the diagonal and thus generating stable self-sustaining activity. We do this by considerably lowering the firing threshold.

Figure 2A shows the probability for $\theta = 5$ ($C_E = 1000, C_I = 250$). This time, the probability crosses the diagonal, indicating that there are stable, self-reproducing activity states. The curve has three important points p^+, p^* , and p^- .

First, the *ignition point* p^+ , defined as

$$p^+ = \min\{p \in (0, 1] \text{ with } P(p) = p\}. \quad (8)$$

Second, the *stable self-reproducing point* p^* , defined as

$$p^* = \min\{p \in (p^+, 1] \text{ with } P(p) = p\}. \quad (9)$$

Third, the *shut-off point* p^- , beyond which all activity ceases again. It is defined as:

$$p^- = \min\{p \in (p^*, 1] \text{ with } P(p) = p^+\}. \quad (10)$$

For $p < p^+$ the firing probability quickly tends to zero, for $p^+ < p < p^*$ the firing probability is amplified, and for $p > p^*$ the probability $P(p)$ quickly tends to zero again. Thus, stable activity is only possible within the range $p^+ < p < p^-$. If too few or too many neurons in the network are active, activity will cease in the next iteration.

In figure 2A we have $p^+ \in (0.0006, 0.0007)$, $p^* \approx 0.11$, and $p^- \in (0.5, 0.6)$. $P(p)$ quickly rises towards its maximum at $p = 0.004$, where the probability is amplified by a factor of 34. It then quickly falls towards zero. Since the activity in the network will move along this curve, we expect the rates in such a network to be volatile. If the activity exceeds the shut-off point $p^- = 0.6$, activity will cease in the next iteration.

Figure 2B demonstrates that the stable point persists, even if we reduce the number of synapses by a factor of 10 ($C_E = 100, C_I = 25, \theta = 5$). The probability still rises above the diagonal and crosses it again at $p^* \approx 0.2$. Decreasing the number of connections has obviously increased the activity at the

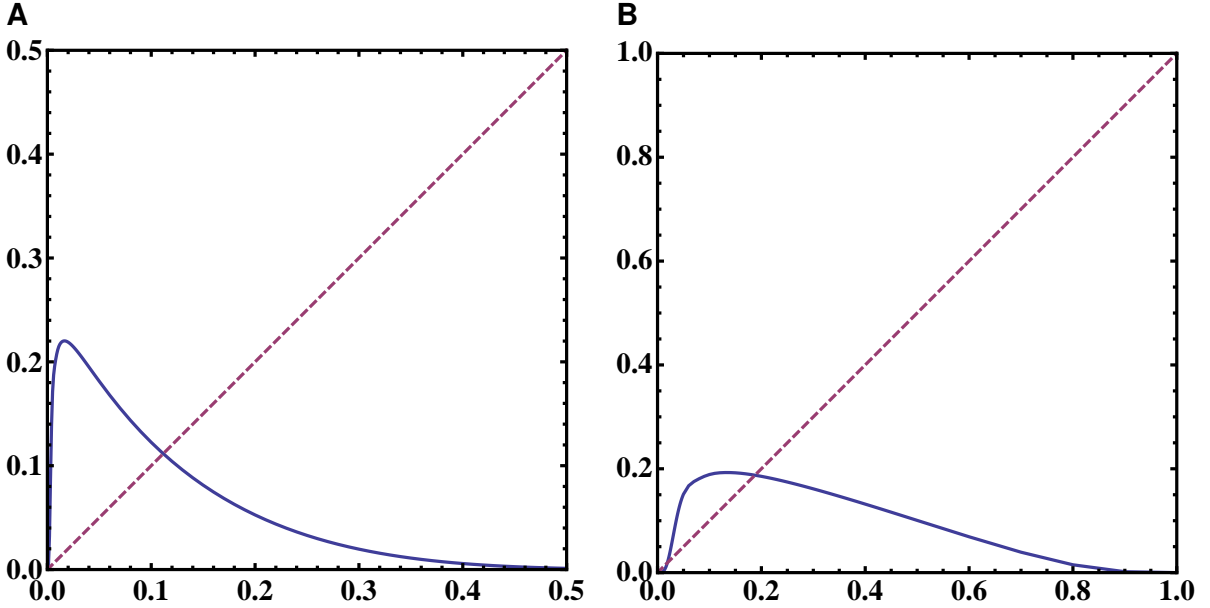


Figure 2. Stable points of the firing probability transfer function (numerical solution of equation (5)) (A) Many synapses, low threshold; $\theta = 5, C_E = 1000, C_I = 250$. The probability steeply rises to its peak at $p = 0.004$, before it falls towards zero again. The intersection with the diagonal at $p^* \approx 0.11$ is a stable fixed point. (B) Low threshold and fewer synapses ($C_E = 100, C_I = 25, \theta = 5$). The curve rises more slowly than in (a) and also falls off more slowly towards zero. The intersection with the diagonal at $p^* \approx 0.2$ is a stable fixed point.

stable point, because with $g = 5 > 1/\gamma$, the synaptic weights decrease more strongly than the number of connections.

Another notable change is the slope of the curve. The probability rises more gently, has a wider peak, and also decreases more slowly, compared to 2A. Thus, we expect the rates in a network with these parameters to be less volatile. Moreover, the shut-off point p^- is beyond 0.9, thus, the network can endure much higher activities without shutting off.

Stability in recurrent neural networks

We now turn from numerical evaluations of the simplified Griffith model to simulations of recurrent networks of current based integrate-and-fire neurons. In these simulations we investigate whether the stable states of self-sustaining activity found in Griffith's model can indeed be induced in networks of spiking neurons.

Neuron and network model

The network model that we will be using is based on the sparse random network by Brunel [13]. It consists of N_E excitatory and N_I inhibitory neurons, with $N_I = \gamma N_E$ and $\gamma = 0.25$.

Each neuron receives input from C_E excitatory and C_I inhibitory neurons, with $C_E = \epsilon N_E$ and $C_I = \epsilon N_I$, where ϵ satisfies $0 \leq \epsilon \leq 1$. The cases $\epsilon = 0$ and $\epsilon = 1$ correspond to an unconnected and a fully connected network, respectively.

We consider integrate-and-fire neurons with current based synapses [24], whose membrane potential

is given by:

$$\tau_m \frac{dV_m^i}{dt}(t) = -V_m^i(t) + R_m I^i(t), \quad (11)$$

for each neuron $i = 1 \dots N = N_E + N_I$, where τ_m is the membrane time constant, R_m the membrane resistance, and $I^i(t)$ the synaptic current. Whenever the membrane potential V_m reaches the threshold value V_{th} , a spike is sent to all post-synaptic neurons.

Each spike induces a post-synaptic current, modeled as alpha functions:

$$psc(t) = \alpha \cdot t \exp\left(-\frac{t}{\tau_{syn}}\right), \quad (12)$$

where α is chosen such that the resulting post-synaptic potential has amplitudes J_E and J_I for excitatory and inhibitory synapses, respectively.

J_{ij} is the efficacy and D_{ij} the delay of the synapse from neuron j to neuron i . Excitatory synapses have efficacy J_E and inhibitory synapses efficacy $J_I = -g \cdot J_E$, with $g > 0$. The parameters g and γ determine the ratio of excitation to inhibition. The regime $g \approx 1/\gamma$ is called the *balanced* regime, $g > 1/\gamma$ the inhibition dominated regime, and $g < 1/\gamma$ the excitation dominated regime.

The details of our model are summarized in the figures 10 and 11.

Relation to Griffith's model

The parameters of Griffith's model are the number of excitatory and inhibitory inputs C_E and C_I , the ratio between excitation and inhibition g , and the threshold θ .

C_E and C_I are determined by the respective number of excitatory and inhibitory neurons, N_E and N_I , as well as the connection probability ϵ .

The threshold θ is given by the membrane threshold V_θ and the excitatory synaptic weight J_E :

$$\theta = V_\theta / J_E \quad (13)$$

Before we turn to stable states of self-sustained activity, we will review the model Brunel [13] which describes how external excitatory spike input can induce low-rate activity in a recurrent network. We use this model as a reference for comparison with the self-sustained states that don't require external input.

Next, we consider the cases of stable self-sustained activity, discussed in the previous section. We will then extend our simulations and investigate how the firing rate and the survival time of self-sustained states depend on the ratio of excitation and inhibition as well as the size of the excitatory synaptic weight J_E .

Brunel's model: many connections, high threshold

In his model of asynchronous irregular activity, Brunel [13] assumed that each neuron has a large number of synapses with accordingly small synaptic weights. In Griffith' terms, these assumptions correspond to the case of many connections with high threshold and we have seen that in this regime, there is no stable activity state except for $p = 0$. To overcome this problem the model is usually supplied with external excitatory input [12, 13] or pacemaker neurons [15, 25].

Figure 3 shows the spiking activity, induced by an external Poisson input, as proposed by Brunel [13]. The configuration corresponds to the case, used in figure 1A and to the *asynchronous irregular state*, shown in figure 8C of [13].

Figure 3A shows a raster plot of the spiking activity of 50 neurons over an epoch of 500 *ms*. Each point in the raster-plot corresponds to a spike of a neuron at the respective time. At time $t = 0$ *ms* all neurons are in the quiescent state. At $t = 50$ *ms* an external Poisson input is switched on and induces spiking activity in the network. The Poisson input then persists for the duration of the simulation. After

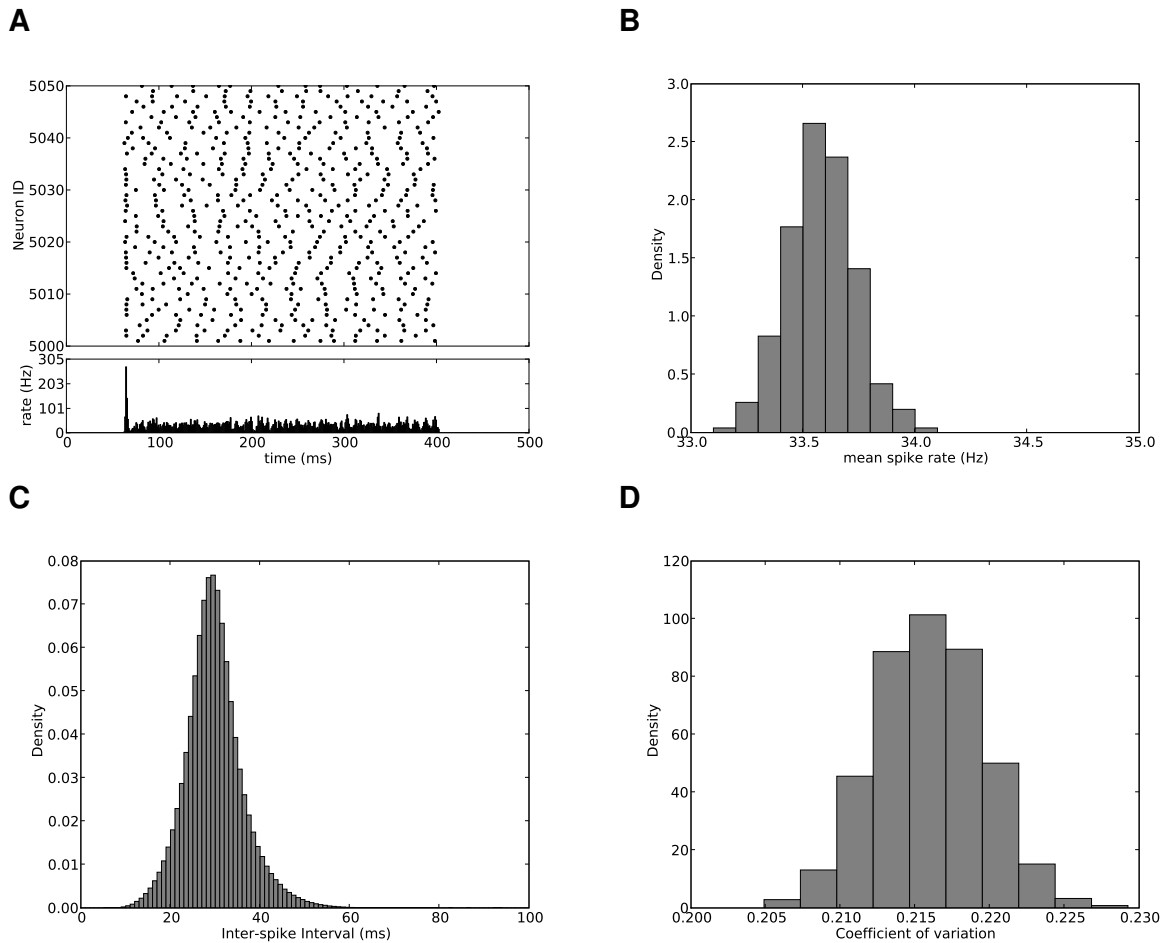


Figure 3. Activity in a random network with 12 500 neurons, $g = 5$, $J = 0.1$, $\epsilon = 0.1$, and Poisson background activity with $\nu_{ext} = 38$ Hz. Panels B-D are computed from simulations that lasted 100 seconds. **(A)** Raster plot (top) and spike count (bottom) of 50 neurons for 500 milliseconds. Poissonian background activity is supplied between $t = 50$ ms and $t = 400$ ms. **(B)** Firing rate distribution of all excitatory neurons. The firing rates are approximately Gaussian distributed within the range of 33 Hz to 34.5 Hz. **(C)** interspike interval distribution. The interspike intervals are Gaussian distributed with a mean of 30 ms and standard deviation of approx. 6 ms. **(D)** Histogram of the coefficient of variation. The coefficients of variation of the interspike intervals are also Gaussian distributed with mean 0.22 and standard deviation 0.004.

an initial transient the network assumes the asynchronous irregular state (AI) [13]. This state is not self-sustaining, because if the Poisson input is switched off at $t = 400 \text{ ms}$ the network falls back into the quiescent state again.

Barbieri and Brunel [18] observed that the spiking activity produced by these types of networks cannot explain the irregularity of experimentally recorded data. This is illustrated in figures 3B-3D.

Figure 3B shows that the firing rates in the network, measured over 100 seconds follow a very narrow Gaussian distribution with mean 33.5 Hz and standard deviation less than 1 Hz. In other words, all neurons fire essentially at the same rate. The small variation of the rates argues against the assumption that each neuron is firing according to a Poisson distribution. Figure 3C confirms this by showing that also the interspike intervals follow a narrow Gaussian distribution ($30 \text{ ms} \pm 6 \text{ ms}$), as opposed to an exponential distribution that would be the signature of Poissonian firing. The coefficients of variation that result from this narrow ISI distribution (Figure 3D) are accordingly small ($CV \approx 0.215 \pm 0.05$). Thus, the neurons in this network behave like oscillators whose period is slightly perturbed.

Self-sustained activity in recurrent networks of integrate-and-fire neurons

Griffith's model predicts that stable self-sustained activity states exist in networks where the firing threshold is sufficiently low. We will first look for these states in simulation. Next we will investigate, how abundant and how robust these self-sustained activity states are. Do they exist only for a very limited set of parameters, or do they exist in a larger region of the parameter space? We will then have a closer look at the firing pattern of self-sustained activity.

Our starting point is the configuration shown in figure 2B. Assuming a firing threshold of $V_{th} = 20 \text{ mV}$, Griffith's model predicts that we can observe stable self-sustained activity with an excitatory synaptic weight of $J_E = 20 \text{ mV}/5 = 4 \text{ mV}$. Indeed, in simulation we found that a network with $J_E = 4 \text{ mV}$ shows self-sustained activity states.

Figure 4 shows the results of a simulation that lasted 100 s. Figure 4A shows the first spiking activity of 50 excitatory neurons during the first 500 ms (top) and the corresponding ensemble rate of 1000 excitatory neurons (bottom). Again, at $t = 0$, all neurons are in the quiescent state. To trigger activity, we stimulated each neuron with weak Poisson noise for a period of $t = 150 \text{ ms}$. After that, no further input was given and the network was left to its own devices.

The noise stimulus causes a transient network response, after which the network settles to a mean rate firing rate of 32 Hz. This state persists until the end of simulation at $t = 100 \text{ s}$. Figure 4B shows the spiking activity after 90 seconds of simulation to illustrate that the self-sustained state is stable.

There are a number of obvious differences between the raster plots of the Brunel network in figure 3 and the raster plots in figure 4. First, the Brunel network is only active with external Poisson input, whereas the network in figure 4 continues to fire even in the absence of external input. This state persists for very long times, in this case 100 seconds. We call this network state the *self-sustained asynchronous irregular* (SSAI) state.

The self-sustained asynchronous irregular state is not stable in the strict mathematical sense, because the random connectivity may cause the number of active neurons to drop below a critical limit and then spiking will stop altogether. Since there is no noise input into the network, it depends on the instantiation of the random connectivity if and when the self-sustained state will stop (see also [11, 16]).

Second, in figure 3 the spikes are relatively homogeneously distributed, whereas in figure 4 the distribution of spikes is very irregular. By contrast, neurons in the SSAI state exhibit large periods with few or no spikes at all, as well as *bursting* periods where spikes are so close together that they can hardly be distinguished. It appears as if the neurons switch between states of high activity and states of silence.

Third, the population rates (lower part of each panel) of the self-sustained networks differ from the Brunel case. In Brunel's case (figure 3), the population rate stays quite constant after the initial transient or it slightly oscillates [26]. By contrast, the population rate of the self-sustained networks in figure 4 show large fluctuations without any obvious temporal structure.

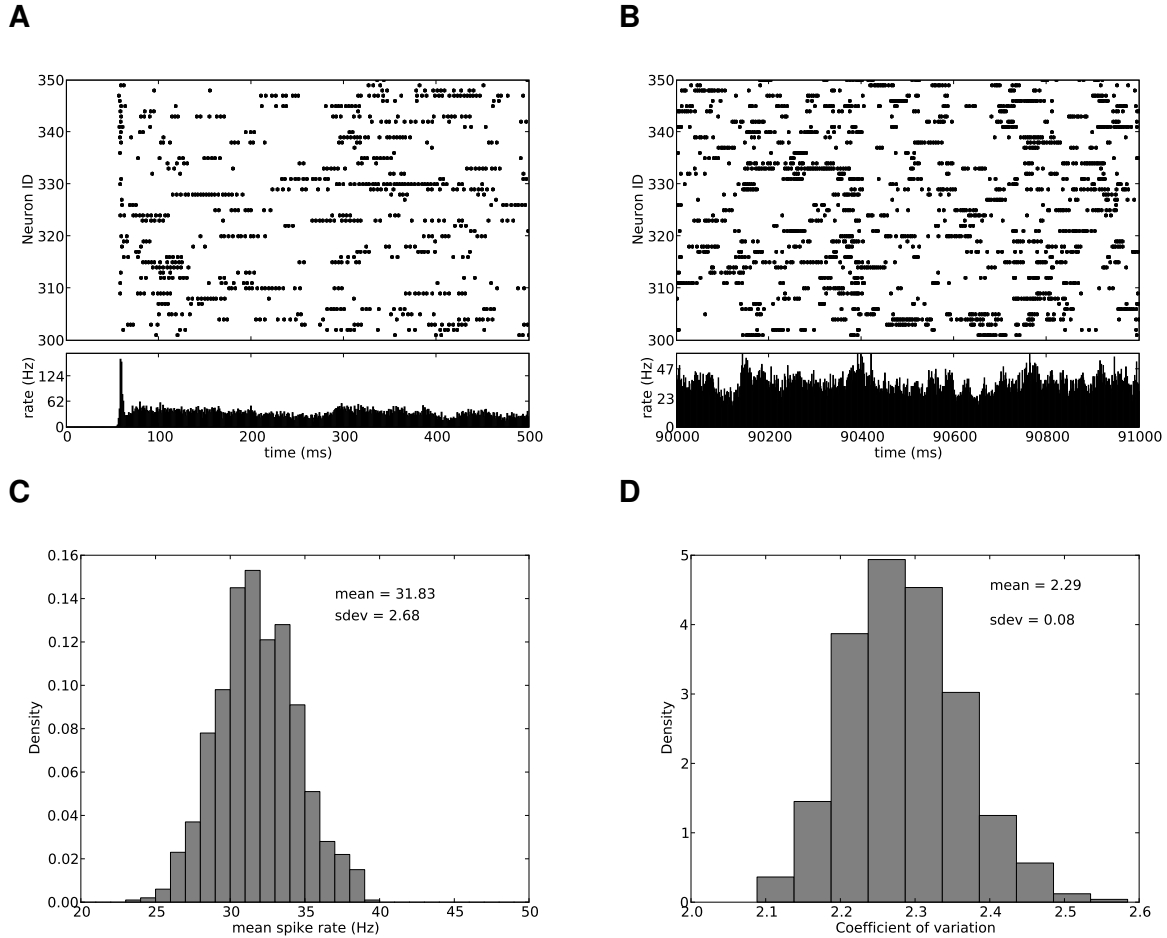


Figure 4. Self-sustained activity in a network of 12,500 neurons. Each panel shows the spiking activity of 50 representative excitatory neurons (top) and the population rate of 1,000 neurons (bottom). **(A)** first 500 ms of a simulation with parameters $g = 5$, $J = 4.0$ mV, $\epsilon = 0.01$ which lasted 100 s. Between $t = 50$ ms and $t = 200$ ms, the neurons were supplied a weak Poisson stimulus to trigger spiking. After that, spiking activity continues for the whole simulation epoch at an average rate of 31.83 Hz. **(B)** Activity of the same network as in A after 90 s. **(C)** Distribution of the mean firing rates of the neurons. The mean firing rates follow a Gaussian distribution with mean $\mu = 31.83$ Hz and standard deviation $\sigma = 2.28$ Hz. **(D)** Distribution of the coefficients of variation (CV) of the interspike interval (ISI) distribution. The CV follows a Gaussian distribution with mean $\mu_{CV} = 2.29$ and standard deviation $\sigma_{CV} = 0.08$. The rate and CV distributions were estimated from the activity of 1,000 neurons, recorded for 100 seconds.

To quantify the irregularity of neuronal activity we looked at the distribution of mean firing rates (figure 4C) as well as the distribution of the coefficients of variation (figure 4D).

For figure 4D, we computed the mean firing rates for 1 000 neurons over the simulation period of 100 seconds. Firing rates are roughly Gaussian distributed with a mean of 31.83 Hz and a standard deviation 2.68 Hz. The lowest firing rate in the population is 20 Hz and the highest rate is 40 Hz.

From figures 4A and 4B we know that over time, the firing rate of each neuron fluctuates considerably. These fluctuations lead to a correspondingly large coefficient of variation (CV), which is the standard deviation of the interspike intervals (ISIs) divided by their mean. Figure 4D shows the distribution of the coefficients of variation of 1 000 neurons. We find a Gaussian distribution with mean 2.29 and standard deviation 0.08. The smallest CV is 2.1 which is more than twice as large as the CV of a Poisson process.

Interspike interval statistics in the SSAI state

Next, we investigate the statistical properties of interspike intervals in the SSAI state. If the neuron were firing Poissonian with rate λ then their interspike intervals should be exponentially distributed:

$$f_{\text{exp}}(t) = \lambda \exp(-\lambda \cdot t) \quad (14)$$

On a logarithmic scale, the exponential distribution is a straight line whose slope is proportional to the rate of the exponential distribution, which is also the rate of the Poisson process:

$$\log_{10}(f_{\text{exp}}(t)) = \log_{10}(\lambda \exp(-\lambda \cdot t)) \quad (15)$$

$$= \log_{10}(\lambda) - \lambda \log_{10}(e) \cdot t \quad (16)$$

$$= a \cdot t + b \quad (17)$$

with $a = -\lambda \log_{10}(e)$ and $b = \log_{10}(\lambda)$.

If the firing patterns in the SSAI state can at least partially be described by a Poisson process, the logarithmic interspike interval distribution should have a linear part.

Figure 5A shows the interspike interval distribution for the network from figure 4 on a logarithmic scale. For intervals larger than 80 ms, the distribution is well described by a straight line with slope $a_{t>80} = -0.0037 \text{ ms}^{-1}$, which corresponds to a firing rate of $\lambda_{t>80} = 8.81 \text{ Hz}$.

Intervalls smaller than 80 ms cannot be explained by this Poisson process. In fact, almost 80% (78.8%) of all spikes contribute to these intervals, although the neurons spend 80% (79.2%) of their time in the remaining intervals larger than 80 ms.

To understand how this surplus of short intervalls is generated, we return to the hypothesis that during SSAI activity the neurons are in one of two states: a low rate state and a high rate state. The low rate state accounts for all intervalls larger than 80 ms, while the high-rate state must account for the surplus of intervals below the threshold.

Under this hypothesis, the interval distribution in figure 5A should be the convolution of two exponential distributions with rates λ_1 and λ_2 .

$$f_{ISI}(t) = f_{\text{exp}1}(t) * f_{\text{exp}2}(t) \quad (18)$$

$$= \frac{\lambda_1 \cdot \lambda_2}{\lambda_1 - \lambda_2} (\exp(-\lambda_2 t) - \exp(-\lambda_1 t)) \quad (19)$$

For $t \cdot \lambda_1 \gg 1$, we get

$$f_{ISI}(t) \approx \frac{\lambda_1 \cdot \lambda_2}{\lambda_1 - \lambda_2} (\exp(-\lambda_2 t)) \quad (20)$$

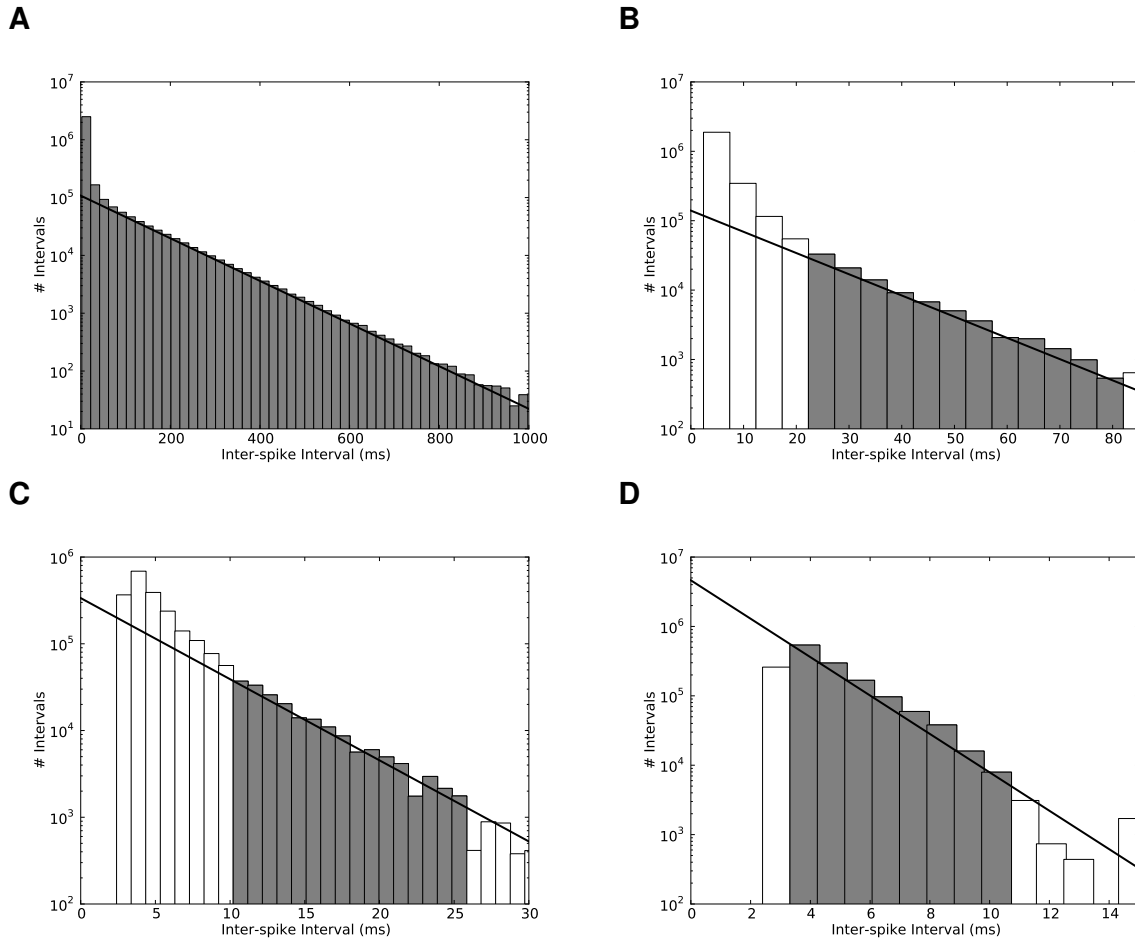


Figure 5. Interspike interval distribution for the network in figure 4 on a logarithmic scale. In each panel, a regression line (black) shows which region of the distribution is well described by an exponential distribution. In panels B-D, only the gray bars were used to determine the regression lines. **(A)** ISI distribution for all intervals smaller than 1 000 *ms*. **(B)** ISI distribution for intervals smaller than 80 *ms*, corrected by the intervals explained by the distribution in panel A. **(C)** ISI distribution for intervals smaller than 30 *ms*, corrected by the intervals explained by the distributions in panels A and B. **(D)** ISI distribution for intervals smaller than 15 *ms*, corrected by the intervals explained by the distributions in panels A through C. See text for details.

No.	range	slope (mHz)	rate (Hz)	\sum time (%)	\sum spikes (%)
1	$3 < t \leq 10$	-0.3415	786.41	4	28
2	$10 < t \leq 25$	-0.1144	263.48	7	37
3	$25 < t \leq 80$	-0.0296	68.20	6	11
4	$80 < t$	-0.0037	8.82	79	21

Table 1. Times scales and firing rates of a network during the SSAI state. The slopes correspond to the regression lines in figure 5.

Using equation (20) we can estimate the slow firing rate component.

We can also estimate the fast firing rate component. To this end, we subtract the expected number of intervals from the slow component, because from equation (19) we know that the interval distribution is basically the sum of the two superimposed distributions. Thus:

$$f_{ISI}(t) - \frac{\lambda_1 \cdot \lambda_2}{\lambda_1 - \lambda_2} \cdot f_{\exp 2}(t) = \frac{\lambda_1 \cdot \lambda_2}{\lambda_1 - \lambda_2} \exp(-\lambda_1 t) \quad (21)$$

Figure 5B shows the ISI distribution for intervals smaller than 80 *ms* with the intervals, generated by the slow rate subtracted. Again, a good part of the distribution is well described by a Poisson process, this time with rate $\lambda_{20 < t < 80} = 68.20$ Hz, but for intervals shorter than 20 *ms*, the model again fails.

We can repeat this procedure again to estimate the rate of the next faster process. This is shown in figures 5 C and 5D.

Altogether we find, that the interval distribution of this network can be described by four Poisson processes with widely different rates, valid for different ranges of interspike intervals.

If the four Poisson processes were active in parallel, it would be impossible to separate them in the interval distribution, because the sum of two or more Poisson processes with rates $\lambda_1, \lambda_2, \dots, \lambda_n$ is again a Poisson process with rate $\lambda_* = \sum_i \lambda_i$. Thus, we must assume that the neurons switch between a small number of Poisson states, each with its own firing rate and its own range of intervals. These states and their interval ranges are summarized in table 1.

The fastest process has a rate of $\lambda_1 = 786.41$ Hz and is responsible for the high-frequency burst with interspike intervals between 3 and 10 *ms*, observed in the raster plots of figure 4. Note that although this rate is larger than the theoretical maximum of $\lambda_{\max} = 1/t_{ref} = 500$. Hz the smallest interval is with 2.4 *ms* still larger than the refractory period of 2 *ms*. The very high rate of λ_1 is the result of the large number of intervals between 3 and 10 *ms*.

The slowest process is responsible for the large gaps between spikes, observed in figure 4 and has a rate of $\lambda_4 = 8.82$ Hz.

Firing rates and survival times depend on J and g

So far we have looked at specific network configurations which were suggested by the discrete Griffith model. We now step up from these specific cases to see how the mean firing rate and the survival time of the self-sustained activity states depend on the ration between excitation and inhibition g and on the synaptic strength J .

To this end, we simulated a network with 10 000 excitatory and 2500 inhibitory neurons for up to 100 seconds for combinations of (g, J) , where g was varied from 3 to 6 in steps of 0.01 and J was varied from 1 *mV* to 5 *mV* in steps of 0.01 *mV*. In each simulation, we measured the mean firing rate of the neurons as well as the survival time of the SSAI state.

The results of these simulations are summarized in figure 6. Figure 6A shows the contour plot of the mean firing rate as a function of J_E and g . Darker colors correspond to lower rates. Along the contour lines, the firing rate remains approximately constant (iso-rate boundaries).

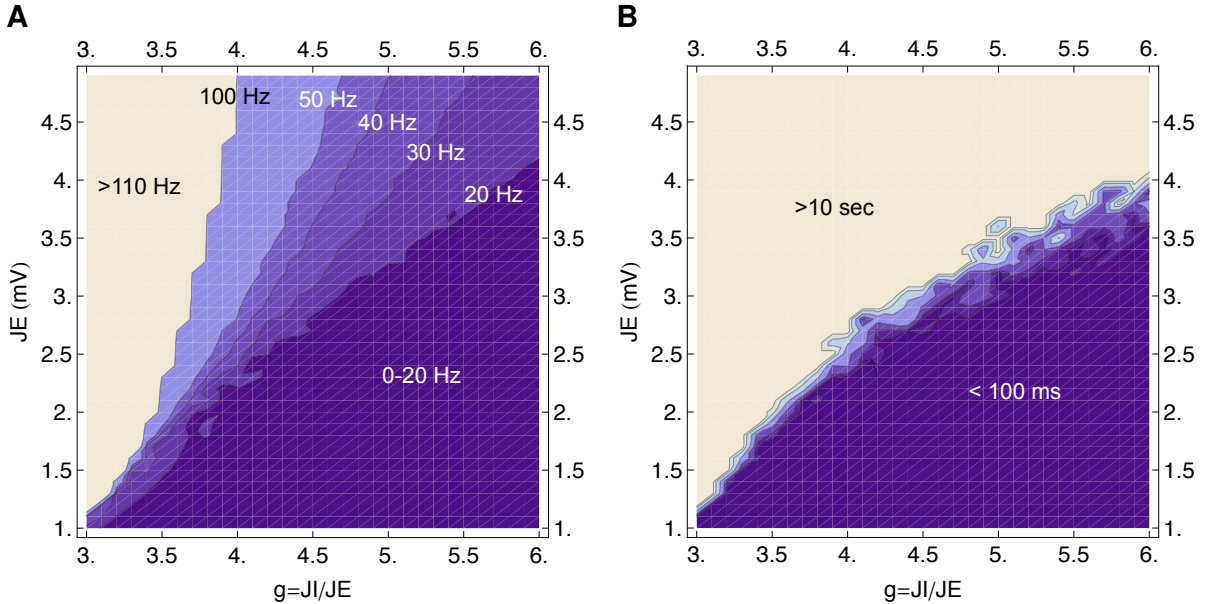


Figure 6. (A) Contour plot of the mean firing rate as a function of J and g . For small g and $J > 1$, the mean rate approaches the maximum $1/t_{ref}$. with increasing g , the mean rate decreases monotonically. The region between 0–20 Hz is characterized by short-lived self-sustained states. Stable self-sustained states can be found for mean rates greater than 20 Hz. (B) Contour plot of the survival time as a function of J and g . There is a sharp transition between immediate network death (blue area) and long survival (beige area) which does not soften significantly with increasing J and g .

The abscissa represents ratio of inhibition to excitation g . For $g = 4$, excitation and inhibition contribute equally to the synaptic current. For $g < 4$, excitation contributes more than inhibition, and for $g > 4$, inhibition contributes more than excitation.

For $g < 3$ the excitatory population dominates the network activity and the firing rates approach the theoretical maximum of $\nu_{max} = 1/t_{ref}$. This is true even for small excitatory amplitudes.

As g increases with the inhibitory amplitude, rates become lower, until they reach the physiologically interesting range of 0–40 Hz. This range is reached even before inhibition balances excitation, however this activity is usually unstable. This is also evident from the very steep transition between the white area of high rates and the dark area of low rates.

With further increasing relative inhibition (larger g), the slope of the transition between high and low rates decreases, creating wide regions of intermediate rates.

Figure 6B shows the survival time of network activity for the same parameter range. Here, we observe a sharp transition between basically two states: either activity ceases after less than 100 ms, or it survives for a very long time. In contrast to the firing rates in figure 6A, the transition remains sharp for all values of the relative inhibition g . This means that SSAI states in inhibition dominated networks ($g > 4$) are more stable than in balanced ($g = 4$) or excitation dominated networks ($g < 4$).

Self-sustained states exist in a wide range of network sizes

Self-sustained asynchronous irregular states are an emergent network property which require a minimal network size. Thus, we were interested in the smallest network which still show SSAI states. We were also interested in larger networks where the number of connections per neuron increases and the synaptic strength becomes smaller relative to the firing threshold.

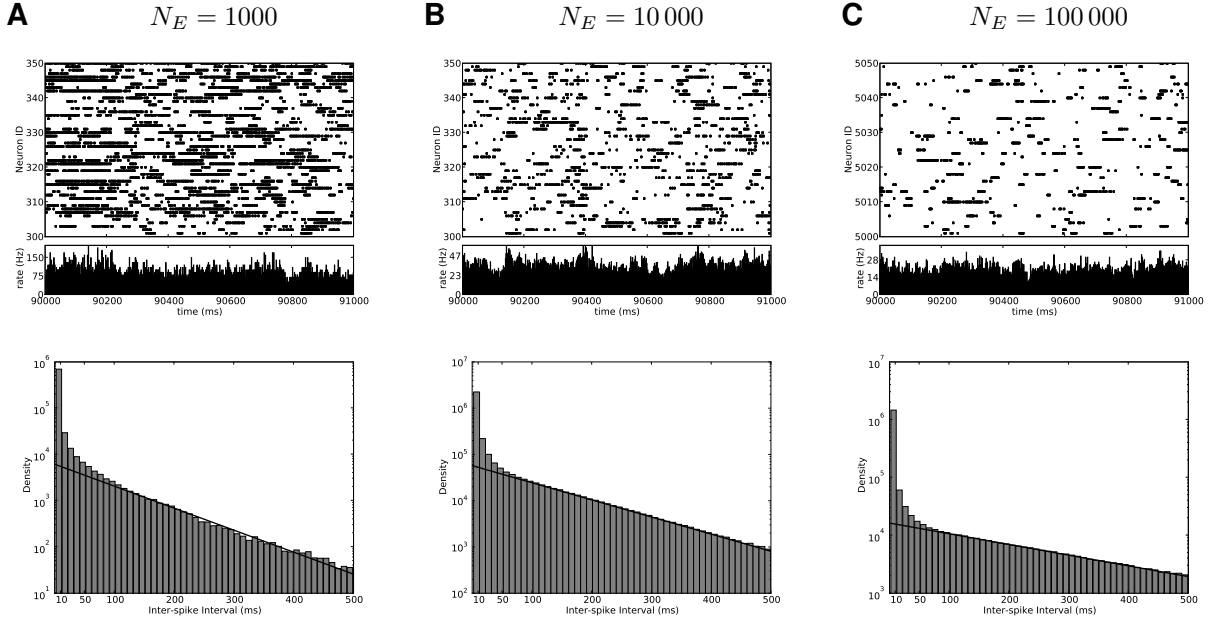


Figure 7. Self-Sustained activity in networks of different sizes. Raster plots of the spiking activity is shown in the top row, the interval distribution in the bottom row. The firing rates decrease with increasing network size. This is also visible from the interval distributions, that shift towards larger intervals. **(A)** 1 000 excitatory and 250 inhibitory neurons, **(B)** 10 000 excitatory and 2 500 inhibitory neurons, and **(C)** 100 000 excitatory and 25 000 inhibitory neurons.

A trivial way of scaling the network is to start with a given configuration (e.g. $N = 10\,000$, $g = 5$, and $J = 3.8\text{ mV}$) and to increase the number of neurons, while keeping the synaptic amplitude J and the numbers of connections C_E and C_I constant. This strategy works well, and yields qualitatively the same results as the original smaller network (not shown). In particular the mean firing rates stay constant.

Alternatively, we can keep the connection probability constant. Then, the number of connections per neuron will grow as the network increases. To compensate for the increasing number of connections, we must decrease the synaptic amplitudes J proportional to $\sqrt{N/N'}$. This scaling works until the synaptic amplitudes become small compared to the threshold.

Similarly, there is a lower limit to the network size. If we reduce the number of neurons for a fixed amplitude J and fixed numbers of connections C_E and C_I , the connectivity ϵ increases accordingly. Thus, we quickly reach the case where ϵ approaches 1 and each neuron receives input from all other neurons. In this state of total symmetry asynchronous irregular states cannot exist.

If we keep the connectivity ϵ constant, we can, in theory, reduce the network size until $\lfloor \epsilon * N \rfloor = 0$. Thus, for $\epsilon = 0.1$ the smallest theoretical network size would be $N = 10$. However, simulations show that already for $\epsilon = 0.1$ and $N = 100$ the self-sustained state requires synaptic amplitudes of $J > \theta$ and shows unphysiological spike trains where each neuron switches between high-frequency bursts and silence. Moreover, the self-sustained state becomes unstable. The main reason seems to be that for such small networks each neuron receives less than 10 inputs, each sufficiently strong to trigger a spike. At the same time, each neuron sees a considerable portion of the entire network. Thus, correlations amplify quickly until coherent down-states stop the network activity. In between these extremes there is a wide range of network sizes and connectivities where self-sustained states of asynchronous irregular activity exist.

Figure 7 shows the raster plots and interval distributions for example networks of three sizes: 1 000, 10 000, and 100 000 excitatory neurons. The network in figure 7A has the highest rate and the largest

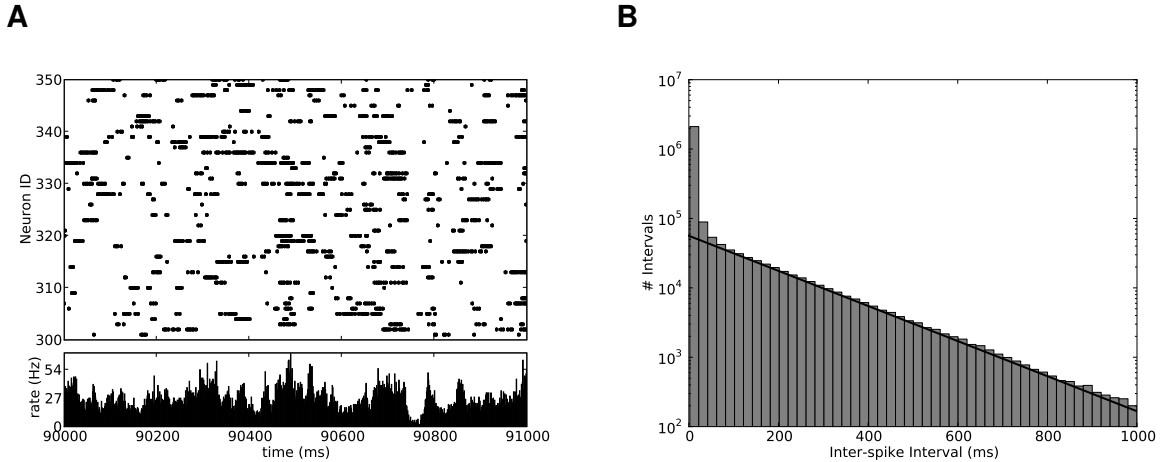


Figure 8. Self-Sustained activity in a network with many weak and few strong synapses. **(A)** Raster plot of spiking activity (top) and population firing rate (bottom). **(B)** ISI-histogram on a logarithmic scale.

PSP amplitude, but the smallest number of connections per neuron.

The networks in figures 7B and 7C have the same synaptic amplitudes and the same connection probability, thus, they differ only in the number of connections per neuron and in the resulting firing rates. Apart from the firing rates, there is no qualitative difference in the raster plots or the interval distributions. The most prominent feature seems to be that small networks are more dominated by small spike intervals than large networks. This is best seen in the interval distribution which widens considerably as the networks become larger.

Few strong synapses in a sea of weak ones

Recently, it has been proposed that cortical networks have a long tailed distribution of synaptic weights, where most connections are very weak, but some connections are very strong [21, 27]. While the strong connections in such network might facilitate self-sustained activity, the larger number of weak connections may destroy these states again. In the following, we tested, whether a network with many weak and a few strong synapses will exhibit self-sustained activity states. To do so, we took the Brunel network of figure 3 and increased the weight of 1% of its connections to $J = 4 \text{ mV}$. The spiking activity of this network is shown in figure 8A and its ISI distribution in figure 8B.

Figure 8A shows the spiking activity after 90 seconds of simulation which means that a Brunel type network which is *doped* with a small number (1%) of strong synapses also shows self-sustained activity. The firing rate in this state is with 26 Hz about 20% lower than in the undoped network.

Figure 8B shows the ISI-distribution on a logarithmic scale, which clearly looks like the ISI distributions of the plain SSAI networks. In the doped network it is also possible to describe the ISI histogram as superposition of different states. Here, the fastest state has a rate of 956 Hz which is assumed for 3% of the time. The slowest state has a rate of 5.85 Hz and accounts for 85% of the time and almost 20% of the spikes.

Obviously, even a small number of strong synapses suffices to change the dynamics of the network. While the undoped Brunel network, shown in figure 3 has a relatively regular dynamics and cannot sustain firing without external input, the doped network exhibits highly irregular activity which is autonomously sustained without external input. This dramatic effect of only a few strong synapses has important implications for learning and plasticity. On the one hand, it can be beneficial, because it is easy to store

information in self-sustained states by facilitating just a tiny fraction of the synapses in a sub-network. On the other hand, this effect can easily disrupt processing, because otherwise silent populations can be easily pushed into a self-sustained activity state.

Discussion

In this paper, we show that self-sustained states of asynchronous irregular activity can be induced in recurrent networks of simple threshold elements, like integrate-and-fire neurons, under the following conditions:

1. a fraction of the connections are sufficiently strong (i.e. $\Theta/J \ll C_E$).
2. a sufficient number of excitatory neurons is activated to trigger the self-sustained activity state.

Condition 1 contradicts the common view that the dense cortical connectivity implies weak connection strengths [13,23]. Even if all connections in a recurrent network are strong, the firing rate will not approach the theoretical limit of $1/\tau_{\text{ref}}$. Moreover, in a network with weak synaptic connections, a small fraction of strong synapses will actually decrease the overall firing rate in the network.

Condition 2 implies that SSAI states can be induced by temporarily lifting the network activity above the ignition point (equation (8)). This can be achieved by supplying either a brief synchronized input to the excitatory neurons or an asynchronous low-rate stimulus over a longer period of time. Once the SSAI state is reached, the ignition stimulus may be switched off and the AI state will persist.

Self-sustained activity as model for ongoing or spontaneous activity

Spontaneous activity in the mammalian nervous systems is marked by low firing rates between 5 and 10 Hz. By contrast, the self-sustained activity states considered here show much higher rates of 20 Hz and more. This raises the question if and how self-sustained states give rise to low-rate spontaneous activity.

There are several possibilities and we will outline the two most probable ones.

Leaking excitation It has been repeatedly shown that weakly coupled networks with random external input shows stable low-rate firing. Thus, the simplest model to explain low rate spontaneous activity, is excitation from a strongly coupled assembly which acts as external drive for a weakly coupled network.

Coupled assemblies Consider a network of many self-sustained networks (assemblies) which are coupled by competitive inhibition such that at any point in time only one or a small fraction of the assemblies can be active. During normal operation, each assembly would be activated for a short time, before activity switches to another assembly. As a result, the average firing rate of the entire network will be much lower than within each of the assemblies.

Self-sustained activity in conductance based networks

The self-sustained activity states described here result from the combinatorics of strong inputs. They do not rely on specific properties of the synapses or the membrane dynamics. Thus, SSAI states will occur under similar conditions in networks of more complex conductance based neurons. Kumar et al. reported self-sustained activity in large networks of conductance based neurons. In their model, they found that the survival time of self-sustained states grows exponentially with the network size. For networks of $1 \cdot 10^4$ neurons, they found a survival time of less than one second.

By applying the reasoning developed in this manuscript, we found that also in networks of conductance based neurons with few strong connections spiking activity persists for very long periods. Figure 9 shows

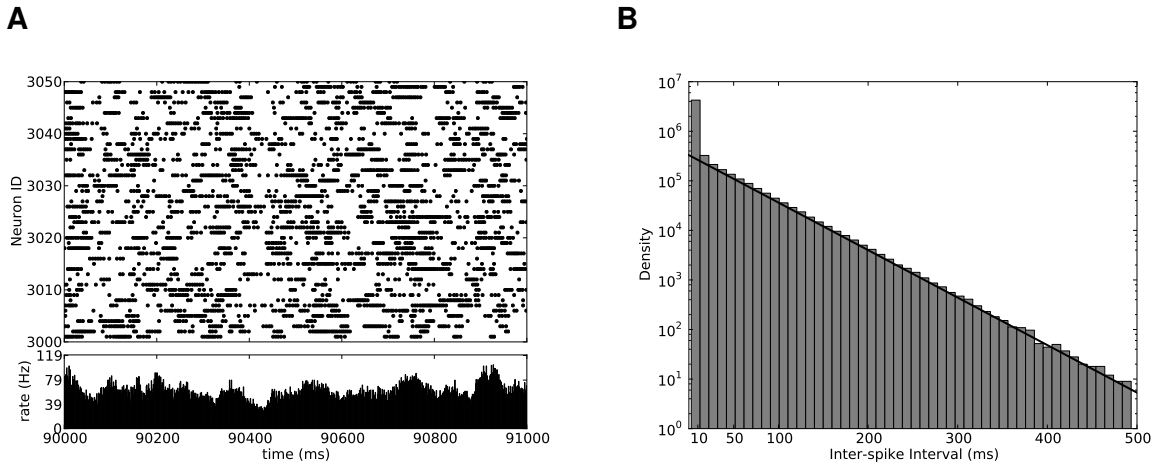


Figure 9. Self-Sustained activity in a network of conductance based neurons. **(A)** Raster plot of spiking activity (top) and population firing rate (bottom). **(B)** ISI-histogram on a logarithmic scale.

the results of a simulation that lasted 100 seconds. Both raster plot (figure 9A) and ISI distribution (figure 9B) look qualitatively identical to that which we found in the current based case. This is a good indication that the arguments and consequences of self-sustained activity, induced by strong synaptic weights also apply to networks of more realistic model neurons or even to networks in the brain.

Variability of firing

It has been argued that the high irregularity of cortical cells is inconsistent with the temporal integration of random EPSPs [17], because such a *counting process* would inevitably be more regular than a Poisson process [2]. This phenomenon can be observed in Brunel’s model in figure 3 [18]. The random superposition of small synaptic weights leads to very regular firing patterns with $CV_i \ll 1$. Several authors have proposed amendments to account for the high irregularity of cortical firing [19,28], by introducing additional mechanisms like different synaptic pathways, synaptic facilitation and depression, or spike-timing dependent plasticity.

In this paper, we demonstrated that none of these mechanisms is actually needed to obtain highly irregular firing. It suffices to take a sparsely connected random network of integrate-and-fire neurons with a small fraction of strong connections. These lead to activity states with $CV_i > 1$, more consistent with the irregularity of experimentally observed ISI distributions [29].

We found that during SSAI activity, the neurons switch between several discrete states which results in the observed high-variability of the ISIs.

Survival and survival time

Kumar et al. [11] observed that the survival time of self-sustained activity states in networks of conductance based neurons grows exponentially with the network size. Networks of 10 000 neurons could sustain firing for as little as 10 ms, while larger networks of 50 000 neurons sustained firing for up to 10 seconds.

By contrast, we observed little dependence of the survival time on the network size. Rather, the networks discussed here show bimodal survival times: Either the activity ceases after a few milliseconds, or it persists for many seconds or minutes (see figure 6B). This was also true for the conductance based network of figure 9 which means that the SSAI state described here is different from the persistent activity described by Kumar et al. [11].

The strong coupling between neurons results in activity which is determined by the combinatorics of the connectivity matrix (the network). Since there is no external source of noise, the response of a given network to a particular stimulus is deterministic. At each point in time a different subset of the connections carries the activity forward. Only if one of these subsets is too small to fulfill the threshold criterion will the activity cease.

Burstiness and multi-state interspike interval distributions

A common measure for burstiness of firing is the surplus of small ISIs (e.g. ISIs < 5 ms) compared to a Poisson process of the same rate [29, 30]. According to this criterion, the firing patterns in SSAI networks is clearly bursty. Moreover, this burstiness is a pure network phenomenon, since the underlying integrate-and-fire neuron model is too simple to produce bursts [31].

We have also shown that bursts in SSAI networks are the signature of different states, each characterised by a different Poisson rate. In total, we observed up to 4 different states (figure 5).

A similar decomposition of interspike interval distributions of experimental data was described by Britvina and Eggermont [32], who showed that the interspike intervals of layer II/III neurons from cat primary auditory cortex can be described by a Markov model, switching between different disjunct states.

Self-sustained activity as memory

Self-sustained activity states do not require very large networks, but can be found in networks larger than about 100 neurons. Moreover, self-sustained states are very stable and persist for many seconds. Thus, a small population of a few hundred neurons could already store information in its activity state, which is very economic compared to other attractor memory models [33]. However, in the presence of strong connections, even small amounts of activity *leaking* into the memory population will trigger the SSAI state, irrespective of a stimulus. This poses a serious problem for models that store information in the activity state of a neural population. To be reliable, such memories need an additional control mechanism which prevents spurious activation of memory populations by the embedding network. Such a control mechanism could be provided by inhibition between different memory pools so that at any time only one or a few memories can be active [34, 35].

Self-sustained activity as signal propagation

In self-sustained networks, the only source of randomness is the connectivity matrix. Once the connectivity is fixed, the activity in the network is deterministic. Consequently, we may describe self-sustained activity as a sequence of activated neuron groups: An initially activated group of neurons G_0 will trigger spikes in another group of neurons G_2 which in turn will activate the group G_3 and so on.

Since the connections are strong, activating G_0 will always result in the same activation sequence

$$G_0 \rightarrow G_1 \rightarrow \dots \rightarrow G_N$$

and a different starting group G'_0 will result in a different activation sequence

$$G'_0 \rightarrow G'_1 \rightarrow \dots \rightarrow G'_N.$$

Thus, we may regard the initially activated neuron group G_0 as a *signal* which propagates through the network.

An alternative interpretation of the self-sustained activity is that of *recalling* a sequence which has previously been stored by an appropriate learning mechanisms.

In this respect, strongly coupled networks differ from other network architectures like weakly coupled networks and synfire chains [23].

In weakly coupled networks, signal propagation is difficult due to the weak connections and the high level of noise [15].

Strongly coupled networks could also be interpreted as an intertwined synfire chain, because both are characterized by a fixed sequence in which neurons are activated. However, there is an important difference: Activity in strongly coupled networks is not only deterministic, it is also chaotic [8]. Thus, changing only one neuron in G_0 will quickly result in an activation sequence $G'_1 \rightarrow G'_2 \rightarrow \dots$ which is distinct from the original activation sequence. By contrast, synfire chains are robust to small variations in their activation sequence [23, 36]. If one or a few neurons are missing or replaced in the initial set G_0 , the divergent/convergent architecture of the synfire chain will *repair* this defect in the subsequent activation stages [37].

Methods

Neuron and network parameters All networks were simulated using a current based integrate-and-fire model where synaptic currents are modeled as alpha functions. The neuron model and network architecture are described in figures 10 and 11 according to the recommendations of Nordlie et al. [38].

Brunel [13] originally used an integrate-and-fire model with delta currents. These lead to instantaneous voltage jumps in response to each spike. In networks with weak synaptic couplings, such as Brunel's network, these discontinuities are smeared out by the noise. In networks with strong synaptic couplings, however, the voltage jumps remain visible in the interval and rate distributions, since most spikes are then bound to the time grid imposed by the synaptic delays. Thus, we used the more realistic alpha-functions as synaptic currents.

Data acquisition Spike data was recorded to file from the first 1000 non-input neurons and analyzed offline. Since the network was connected as a random graph, we could record from a consecutive range of neurons without introducing a measurement bias.

Spike data For each neuron i , we record the sequence of spike times $S_i = \{t_1, t_2, \dots\}_i$ over an observation interval T . Unless stated otherwise, the observation interval was 100 s. In the following, we write spike-trains as

$$s_i(t) = \sum_{t' \in S_i} \delta(t - t') \quad (22)$$

Firing rates The average firing rate of a neuron i was determined by dividing the total number of spikes n_i within the observation interval T by its duration:

$$n_i = \int_T s_i(t') dt' \quad (23)$$

$$\langle \nu_i \rangle = \frac{n_i}{T} \quad (24)$$

Since there is no noise disturbing the neurons, each independent simulation run (trial) yields the same spike trains. The random connectivity, however, allows us to interpret different neurons as independent realizations of the same random process. Thus, the instantaneous population rate is a good approximation of the average instantaneous firing rate of a neuron.

We computed the population rate, by summing the spikes of all observed neurons within a $\Delta T = 1$ ms window around the time of interest:

$$\nu_N(t, \Delta t) = \frac{1}{N} \sum_{i=1}^N \int_t^{t+\Delta t} s_i(t') dt' \quad (25)$$

A Model Summary			
Populations	Three: excitatory, inhibitory, external input		
Topology	—		
Connectivity	Random convergent connections with probability $P = 0.1$ and fixed in-degree of $C_E = PN_E$ and $C_I = PN_I$.		
Neuron model	Leaky integrate-and-fire, fixed voltage threshold, fixed absolute refractory time (voltage clamp)		
Channel models	—		
Synapse model	α -current inputs		
Plasticity	—		
Input	Independent fixed-rate Poisson spike trains to all neurons		
Measurements	Spike activity		
B Populations			
Name	Elements	Size	
E	laf neuron	$N_E = 4N_I$	
I	laf neuron	N_I	
E_{ext}	Poisson generator	$C_E(N_E + N_I)$	
C Connectivity			
Name	Source	Target	Pattern
EE	E	E	Random convergent $C_E \rightarrow 1$, weight J , delay D
IE	E	I	Random convergent $C_E \rightarrow 1$, weight J , delay D
EI	I	E	Random convergent $C_I \rightarrow 1$, weight $-gJ$, delay D
II	I	I	Random convergent $C_I \rightarrow 1$, weight $-gJ$, delay D
Ext	E_{ext}	$E \cup I$	Non-overlapping $C_E \rightarrow 1$, weight J , delay D
D Neuron and Synapse Model			
Name	iaf_psc_alpha (NEST 2.0)		
Type	Leaky integrate-and-fire, α -current input		
Membrane potential	$\tau_m \dot{V}_m(t) = -V_m(t) + R_m I(t) \quad \text{if not refractory } (t > t^* + \tau_{rp})$ $V_m(t) = V_r \quad \text{while refractory } (t^* < t \leq t^* + \tau_{rp})$ $I(t) = \frac{\tau_m}{R_m} \sum_i w \delta(t - (\tilde{t} + D))$		
Spiking	If $V_m(t-) < V_\theta \wedge V_m(t+) \geq V_\theta$ <ol style="list-style-type: none"> set $t^* = t$ emit spike with time-stamp t^* 		
Synaptic current	$I_{syn} = J \frac{e}{\tau_{syn}} \cdot t \cdot \exp\left(-\frac{t}{\tau_{syn}}\right)$		
E Input			
Type	Description		
Poisson generators	Fixed rate ν_{ext} , C_E generators per neuron, each generator projects to one neuron.		
F Measurements			
Spike times of all neurons.			

Figure 10. Model description according to [38], part 1.

G					
Network Parameters					
Parameter	Network configuration				
	Figure 3	Figure 4, 5, 7B	Figure 7A	Figure 7C	Figure 8
Number of excitatory neurons N_E	10 000	10 000	1000	100 000	10 000
Number of inhibitory neurons N_I	2 500	2 500	250	25 000	2 500
Excitatory synapses per neuron C_E	1 000	100	10	1 000	1 000
Inhibitory synapses per neuron C_I	250	25	2	250	250

G					
Neuron Parameters					
Parameter	Network configuration				
	Figure 3	Figure 4, 5, 7B	Figure 7A	Figure 7C	Figure 8
Membrane time constant τ_m/ms	30	30	30	30	30
Refractory period τ_{rp}/ms	2	2	2	2	2
Firing threshold V_{th}/mV	20	20	20	20	20
Membrane capacitance C_m/pF	1	1	1	1	1
Resting potential V_E/mV	0	0	0	0	0
Reset potential V_{reset}/mV	10	0.0	0.0	0.0	10
Excitatory PSP amplitude J_E/mV	0.1	6.8	3.7	2.7	0.1, 4.0
Ratio $g = J_I/J_E$	5	5	5	4	5
Synaptic delay D/ms	1.5	1.5	1.5	1.5	1.5
Synaptic time constant τ_{sym}/ms	0.5	0.5	0.5	0.5	0.5
Stimulus rate ν_{ext}/s^{-1}	2.0	2.0	2.0	2.0	2.0
Stimulation period (ms)	50–	50 – 200	50 – 200	50 – 200	50 – 200

Figure 11. Model description according to [38], part 2.

The refractory period of 1 ms ensures that each neuron contributes at most one spike to the population rate.

Rate distribution To compute the distribution of firing rates, we first compute the average firing-rate of each neuron according to 24 and then construct a histogram with bin-size $\Delta r = 1$ Hz from the set of all firing-rates:

$$H_\nu(r, \Delta r) = \frac{1}{N} \sum_{i=1}^N \int_r^{r+\Delta r} \delta(\nu_i - r') dr' \quad (26)$$

ISI distribution Given the ordered sequence of spike times S_i of neuron i , we construct the set of interspike intervals as:

$$ISI_i = \{t_2 - t_1, t_3 - t_2, \dots\}_i = \tau_1, \tau_2, \dots, \tau_{\#(ISI_i)_i} \quad (27)$$

The ISI distribution was then constructed by counting the number of intervals that fall in consecutive 1 ms bins in a histogram. To improve the statistics of the histogram, we combined the intervals of all recorded neurons.

$$H_{ISI,i}(isi, \Delta isi) = \frac{1}{\#(ISI_i)} \sum_{\tau \in ISI_i} \int_{isi}^{isi+\Delta isi} \delta(\tau - \tau') d\tau' \quad (28)$$

$$H_{ISI}(isi, \Delta isi) = \frac{1}{N} \sum_{i=1}^N H_{ISI,i}(isi, \Delta isi) \quad (29)$$

CV distribution To compute the CV distribution, we first computed the ISI distributions for each neuron i individually, according to the procedure described above. We then determined the coefficients

of variation for each neuron i according to:

$$CV_i = \frac{\sqrt{\langle ISI_i^2 \rangle - \langle ISI_i \rangle^2}}{\langle ISI_i \rangle} \quad (30)$$

Simulation and analysis All simulations were done with the Neural Simulation Tool NEST [39], using its Python interface pyNEST [40]. The simulation data was written to disk and analyzed off-line, using the NumPy and SciPy libraries for Python (see <http://www.scipy.org> and <http://www.python.org>).

Acknowledgements

The author would like to thank Gaute Einevoll, Håkon Enger, Morits Helias, Edgar Körner, Birgit Kriener, Arvind Kumar, Hans-Ekkehard Plesser, and Tom Tetzlaff for discussions and comments.

References

1. Arieli A, Sterkin A, Aertsen A, Grinvald A (1996) Dynamics of ongoing activity: explanation of the large variability in evoked cortical responses. *Science* 273: 1868.
2. Shadlen MN, Newsome WT (1998) The variable discharge of cortical neurons: implications for connectivity, computation, and information coding. *The Journal of neuroscience : the official journal of the Society for Neuroscience* 18: 3870–96.
3. Tsodyks MV, Kenet T, Grinvald A, Arieli A (1999) The spontaneous activity of single cortical neuron depends on the underlying global functional architecture. *Science* 286: 1943–1946.
4. Fukushima M, Saunders RC, Leopold Da, Mishkin M, Averbeck BB (2012) Spontaneous high-gamma band activity reflects functional organization of auditory cortex in the awake macaque. *Neuron* 74: 899–910.
5. Beurle RL (1956) Properties of a Mass of Cells Capable of Regenerating Pulses. *Philosophical Transactions of the Royal Society of London Series B, Biological Sciences (1934-1990)* 240: 55–94.
6. Ashby WR, Von Foerster H, Walker CC (1962) Instability of Pulse Activity in a Net with Threshold. *Nature* 196: 561–562.
7. Abeles M (1982) *Local Cortical Circuits: An Electrophysiological Study*. Berlin, Heidelberg, New York: Springer Verlag.
8. van Vreeswijk C, Sompolinsky H (1996) Chaos in Neuronal Networks with Balanced Excitatory and Inhibitory Activity. *Science* 274: 1724–1726.
9. van Vreeswijk C, Sompolinsky H (1998) Chaotic balanced state in a model of cortical circuits. *Neural computation* 10: 1321–71.
10. Kuhn A, Aertsen A, Rotter S (2004) Neuronal integration of synaptic input in the fluctuation-driven regime. *The Journal of neuroscience : the official journal of the Society for Neuroscience* 24: 2345–56.
11. Kumar A, Schrader S, Aertsen A, Rotter S (2008) The high-conductance state of cortical networks. *Neural computation* 20: 1–43.

12. Amit D, Brunel N (1997) Model of global spontaneous activity and local structured activity during delay periods in the cerebral cortex. *Cerebral cortex* (New York, NY : 1991) 7: 237–52.
13. Brunel N (2000) Dynamics of sparsely connected networks of excitatory and inhibitory spiking neurons. *Journal of computational neuroscience* 8: 183–208.
14. Latham PE, Nirenberg S (2004) Computing and stability in cortical networks. *Neural computation* 16: 1385–412.
15. Vogels T, Abbot LF (2005) Signal propagation and logic gating in networks of integrate-and-fire neurons. *Journal of Neuroscience* 25: 10786–10795.
16. Destexhe A (2009) Self-sustained asynchronous irregular states and Up-Down states in thalamic, cortical and thalamocortical networks of nonlinear integrate-and-fire neurons. *Journal of computational neuroscience* 27: 493–506.
17. Softky WR, Koch C (1993) The highly irregular firing of cortical cells is inconsistent with temporal integration of random EPSPs. *The Journal of neuroscience : the official journal of the Society for Neuroscience* 13: 334–50.
18. Barbieri F, Brunel N (2008) Can attractor network models account for the statistics of firing during persistent activity in prefrontal cortex? *Frontiers in neuroscience* 2: 114–22.
19. Barbieri F, Brunel N (2007) Irregular persistent activity induced by synaptic excitatory feedback. *Frontiers in computational neuroscience* 1: 5.
20. Griffith JS (1963) On the stability of brain-like structures. *Biophysical journal* 3: 299–308.
21. Song S, Sjöström PJ, Reigl M, Nelson S, Chklovskii DB (2005) Highly nonrandom features of synaptic connectivity in local cortical circuits. *PLoS biology* 3: e68.
22. Braitenberg V, Schüz A (1991) *Anatomy of the cortex: Statistics and geometry*. Springer-Verlag, Berlin .
23. Abeles M (1991) *Corticonics: Neural circuits of the cerebral cortex*, volume 1st edition. Cambridge Univ Press, 1 edition, 294 pp. doi:10.2277/0521376173. URL http://www.cambridge.org/gb/knowledge/isbn/item1137967/?site_locale=en_GB.
24. Tuckwell HC (1988) *Introduction to Theoretical Neurobiology: Volume 1, Linear Cable Theory and Dendritic Structure*. Cambridge University Press Cambridge, UK, 304 pp.
25. Latham PE, Richmond B, Nelson P, Nirenberg S (2000) Intrinsic dynamics in neuronal networks. I. Theory. *Journal of Neurophysiology* 83: 808.
26. Kriener B, Tetzlaff T, Aertsen A, Diesmann M, Rotter S (2008) Correlations and population dynamics in cortical networks. *Neural computation* 20: 2185–226.
27. Teramae JN, Tsubo Y, Fukai T (2012) Optimal spike-based communication in excitable networks with strong-sparse and weak-dense links. *Scientific reports* 2: 485.
28. Barak O, Tsodyks MV (2007) Persistent activity in neural networks with dynamic synapses. *PLoS computational biology* 3: e35.
29. Compte A, Constantinidis C, Tegner J, Raghavachari S, Chafee MV, et al. (2003) Temporally irregular mnemonic persistent activity in prefrontal neurons of monkeys during a delayed response task. *Journal of neurophysiology* 90: 3441–54.

30. Kaneoke Y, Vitek JL (1996) Burst and oscillation as disparate neuronal properties. *Journal of neuroscience methods* 68: 211–23.
31. Gerstner W, Kistler W (2002) *Spiking neuron models: Single neurons, populations, plasticity*. August. Cambridge, U.K.: Cambridge University Press, 480 pp.
32. Britvina T, Eggermont JJ (2007) A Markov model for interspike interval distributions of auditory cortical neurons that do not show periodic firings. *Biological cybernetics* 96: 245–64.
33. Roudi Y, Latham PE (2007) A balanced memory network. *PLoS computational biology* 3: 1679–700.
34. Deco G, Rolls ET (2005) Neurodynamics of biased competition and cooperation for attention: a model with spiking neurons. *Journal of neurophysiology* 94: 295–313.
35. Renart A, Moreno-Bote R, Wang X, Parga N (2007) Mean-driven and fluctuation-driven persistent activity in recurrent networks. *Neural computation* 19: 1–46.
36. Diesmann M, Gewaltig MO, Aertsen A (1999) Stable propagation of synchronous spiking in cortical neural networks. *Nature* 402: 529–33.
37. Gewaltig MO, Diesmann M, Aertsen A (2001) Propagation of cortical synfire activity: survival probability in single trials and stability in the mean. *Neural networks : the official journal of the International Neural Network Society* 14: 657–73.
38. Nordlie E, Gewaltig MO, Plesser HE (2009) Towards reproducible descriptions of neuronal network models. *PLoS computational biology* 5: e1000456.
39. Gewaltig MO, Diesmann M (2007) NEST (NEural Simulation Tool). *Scholarpedia* 2: 1430.
40. Eppler JM, Helias M, Diesmann M, Muller E, Gewaltig MO (2008) PyNEST: a convenient interface to the NEST simulator. *Frontiers in Neuroinformatics* 2: 1–12.